Supporting Information

How Trap States Affect Charge Carrier Dynamics of CdSe and InP Quantum Dots. Visualization through Complexation with Viologen

Anoop Thomas, K. Sandeep, Sanoop Mambully Somasundaran and K. George Thomas[*]

School of Chemistry, Indian Institute of Science Education and Research Thiruvananthapuram (IISER-TVM), Vithura, Thiruvananthapuram, 695 551, India.

E-mail: *kgt@iisertvm.ac.in

	Table of contents	Page No.

1. Experimental methods

The following chemicals, indium acetate (99.99%), myristic acid (99%), and octadecene (technical grade), were purchased from Sigma Aldrich and tris(trimethylsilyl)phosphine (10% by weight in hexane) from Strem Chemicals. All the chemicals were used as received.

All the photophysical experiments were carried out at room temperature in a quartz cuvette having a path length of 1 cm (make Starna, USA), except for femtosecond transient absorption studies. Absorption spectra were recorded on UV-vis-NIR spectrophotometer (model Shimadzu UV-3600). The emission and excitation spectra were recorded using the Horiba Jobin Yvon-Fluorolog 3 spectrofluorimeter. All steady state emission studies were carried out by exciting the solution at 400 nm keeping the excitation as well as emission slit widths at 2 nm.

1.1. Time correlated single photon counting (TCSPC) measurements: Emission lifetimes were measured using picosecond time correlated single photon counting system (model Horiba Jobin Yvon-IBH). Solutions were excited at 405 nm using a pulsed diode laser (NanoLED-405L; <100 ps pulse width and the repetition rate was fixed at 250 KHz). The detection system consist of a microchannel plate detector (model Hamamatsu R3809U-50) having an instrument response time of 38.6 ps, coupled to a monochromator (5000M) and TCSPC electronics (Data station Hub including Hub-NL, NanoLED controller). The luminescence lifetime values were evaluated using DAS6.3 fluorescence decay analysis software. The fluorescent decay curve was fitted with triexponential decay fit. The goodness of fit was judged by χ^2 (1 ± 0.2) values and residual plot. The average lifetime (τ_{avg}) of the QDs in the presence and absence of DV^{2+} was analyzed using the Equation S1,

$$\tau_{avg} = \frac{\alpha_1\tau_1^{\,2} + \alpha_2\tau_2^{\,2} + \alpha_3\tau_3^{\,2}}{\alpha_1\tau_1 + \alpha_2\tau_2 + \alpha_3\tau_3} \qquad \text{(S1)}$$

where τ is the lifetime and α is the pre-exponential factor with subscripts 1, 2 and 3 representing various species.

1.2. Femtosecond transient absorption studies:

Femtosecond transient absorption studies were done at the experimental condition wherein QDs form a 1:1 complex with DV^{2+} ($\lambda = 1$). These experiments can provide information on how the depth of trap states in QDs influence the dynamics of charge carrier recombination.

A Ti.Saphire laser system (Spectra-physics Tsunami Oscillator, 80 MHz, 800 nm) was used as seed for a regenerative amplifier (Spectra-Physics Spitfire, 1 KHz, 4 mJ) for the femtosecond transient absorption studies. The 800 nm output pulse from the regenerative amplifier was split in two parts with a 3:1 beam splitter. By frequency-doubling, one part of the amplified output in the BBO crystal the pump pulse (400 nm) was generated. The pump power was controlled using a series of neutral-density filters and was focused (beam diameter of 300 μm) at the sample placed in a rotating quartz sample cell with 400 μm path length. By focusing the residual part of the amplified beam (800nm, ~1 μJ) on a rotating CaF_2 plate, a white light continuum (WLC) from 420 to 800 nm was generated. The WLC was split into a probe and reference laser beams. The probe beam was focused with a convex lens onto the sample (with a beam diameter of 30 μm). Both the reference and probe beams were focused into a fiber optics-coupled multichannel spectrometer with a dual diode array detector with a 200 nm detection window. The intensity of the reference beam was used to correct the pulse-to-pulse fluctuation of the white-light continuum. A motorized delay stage was used to control the delay time between the pump and probe pulses. The instrument response function (IRF) was determined by measuring solvent responses under the same experimental conditions (10% benzene in methanol). The IRF was found to be ~120 fs.

1.3. Nanosecond laser flash photolysis experiments were carried out using an Applied Photophysics Model LKS-60 Laser Spectrometer using the third harmonic (355 nm, ~70 mJ/pulse) of a Qunta Ray INDI-40 series pulsed Nd:YAG laser with a pulse duration of 8 ns.

1.4. Zeta potential (ζ) of the QDs was analyzed using the Zetasizer Nanoseries (M3-PALS) Malvern-ZEN 3600. ζ values were measured in toluene using the Huckel approximation, as an average of 5 measurements and in all cases the deviation was 1.0 mV.

1.5. HRTEM of samples was prepared by drop casting 100 μL of the QD solution on a carbon coated Cu grid. The solvent was allowed to evaporate. The specimens were investigated with a FEI TECNAI 30 G^2 transmission electron microscope operated at an acceleration voltage of 300 kV.

2. Synthesis of decyl viologen dibromide (DV^{2+})

DV^{2+} was synthesized by refluxing a mixture of 4,4′−bipyridyl (1 mmol, 156.2 mg) and 1-bromodecane (6 mmol, 1.2 mL) in acetonitrile (20 mL) for 24 h at 78 ^{o}C under inert atmosphere. The precipitate obtained was washed several times with hexane and filtered and dried under vacuum. ^{1}H NMR (500 MHz, CD_3OD): d (ppm) 8.65 (d, 4H); 7.60(d, 4H); 3.73 (t, 4H); 1.33 (m, 28H); 0.96 (t, 6H); 1.77 (m, 4H).

3. Synthesis of quantum dots (QDs)

3.1. InP QDs

Myristic acid capped InP QDs were synthesized as follows. Indium acetate (0.4 mmol, 0.110 g) and myristic acid (1.54 mmol, 0.35g) in octadecene (5 mL) was heated to 120 ^{o}C in a three necked round bottom flask equipped with a thermometer under nitrogen atmosphere. The reaction mixture was maintained under vacuum for 90 min at 120 ^{o}C and the further heated to 280 ^{o}C under argon atmosphere. Maintaining the temperature at 280 ^{o}C, a solution of tris(trimethylsilylphosphine) (0.2 mmol, 58 μL) in octadecene (1 mL) was injected resulting in the formation of InP quantum dots. The QDs were precipitated by the addition of a mixture (1:4 by volume) of methanol and acetone and the subsequent centrifugation yielded InP QDs. The residue was redispersed in hexane. The purification procedure was repeated thrice and used further studies.

3.2. CdSe QDs

CdSe QDs were synthesized as follows. A pot mixture containing CdO (0.07 g, 0.5 mmol), dodecylamine (3.8 g, 20.72 mmol), tetradecylphosphonic acid (0.40 g, 1.5 mmol) and octadecene (4 mL) was heated to 300 °C under vacuum, until CdO dissolves completely to produce an optically clear solution. At this temperature, an injection mixture containing TOPSe (selenium

powder in TOP, 83 µL, 0.08 mmol) in TOP (5.2 mL, 2.5 mmol) was injected. After the desired crystal growth, the reaction was arrested by cooling to room temperature. The QDs thus obtained was purified by repeated precipitation (3 times) with methanol. The precipitate was then redispersed in toluene and used for further studies.

4. EDX and XRD analysis of QDs

The crystallinity and size of the QDs are established using X-ray diffraction (XRD) and transmission electron microscopic (TEM) analysis (Figures 1 and S1, Table 1). The size of QDs obtained from the TEM measurements is in close agreement with the calculated values from XRD data, using Scherer equation.[1] EDX measurements confirm the presence of In and P in QDs and rule out the presence of any other impurities (Figure S1)

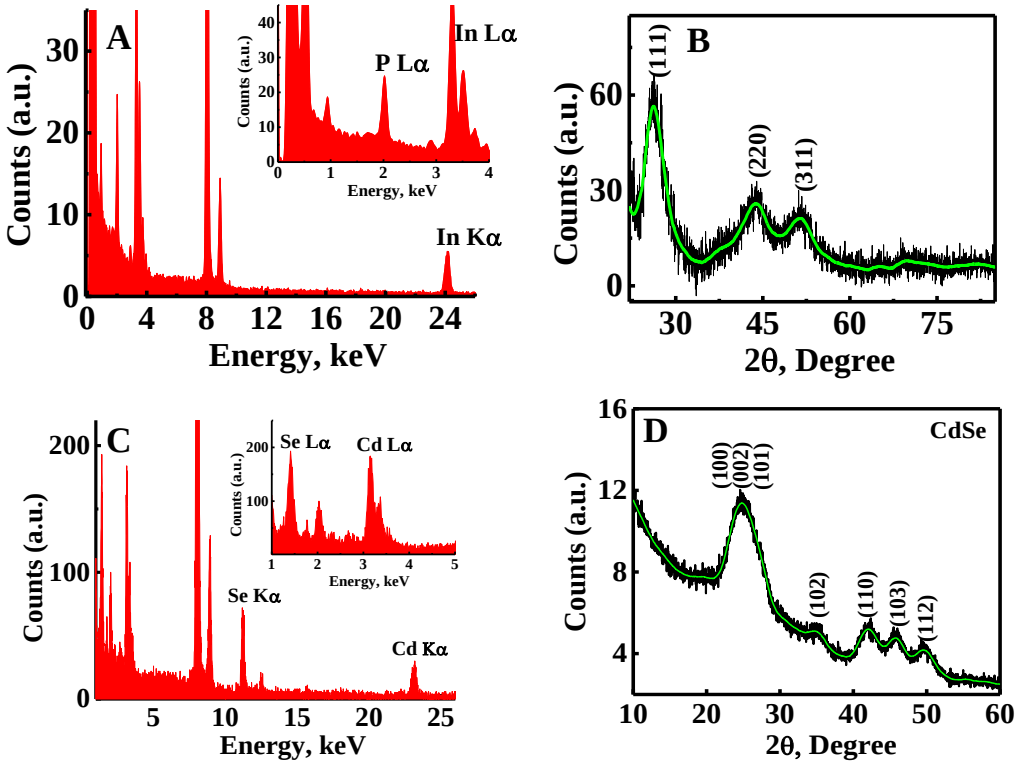

Figure S1. EDX spectrum of (A) InP QDs and (C) CdSe QDs. XRD spectrum of (B) InP QDs and (D) CdSe QDs**.**

5. Determination of InP concentration from ICP analysis

The particle concentration of InP QDs and the corresponding molar extinction coefficient (2.6 x 10^5 $M^{-1}cm^{-1}$ at 548 nm**)** were estimated using Inductively Coupled Plasma (ICP) analysis combined with TEM and UV-vis spectrophotometry. Details are provided below.

Mass % of In obtained from ICP analysis (C_{In}) = 2640 mg L^{-1}

Mass % of P obtained from ICP analysis (C_P) = 492 mg L^{-1}

Ratio of In to P = 1.45

Size of the particle *d* (from TEM) = 36 Å

Lattice constant of InP[2], *a* = 5.83 Å

(Note: InP crystallizes in cubic zinc blende structure with a lattice constant[2](*a*) of 5.83 Å with 8 atoms in unit cell (4 In and 4 P))

Total number of atoms in a nanocrystal[3] (A) = $A = \frac{4}{3}\pi\left(\frac{d}{2}\right)^3 * \left(\frac{8}{V_{Unit\,cell}}\right)$ = 985

Concentration of InP nanocrystal[3] (C_{InP}) = $C_{InP} = \frac{1}{A}\left(\frac{C_{In}}{M_{In}} + \frac{C_P}{M_P}\right)$ = 39.4 μM

(based on ICP)

Extinction coefficient at 548 nm = 2.6 x 10^5 $M^{-1}cm^{-1}$

6. Conduction band and valence band position of QDs

As reported earlier[4,5] the shift in conduction band (CB) and valence band (VB) position of InP QDs were calculated using the following equation,

$$\Delta E_{CB} = \Delta E_{con}\left(\frac{m_h^*}{m_h^* + m_e^*}\right) \qquad \text{S2}$$

where ΔE_{CB} is the energy change of the conduction band, ΔE_{con} is the total confinement energy (E_{1S} - E_g), where E_{1S} is the lowest energy excitonic transition of the QDs (2.07 eV for InP and 2.14 eV for CdSe) and E_g is the bulk band gap of QDs (1.35 eV for InP and 1.7 eV for CdSe), m_h* and m_e* are the hole ($0.65m_e$ for InP and 0.44 m_e for CdSe) and electron ($0.073m_e$ for InP and $0.13m_e$ for CdSe) effective masses, respectively.

7. Free energy change for electron transfer

The driving force for photoinduced electron transfer (ΔG^0) was calculated according to the Weller equation,

$$\Delta G^0 = E_{ox}(D) - E_{red}(A) - E_{00} + e^2/\varepsilon_s d_{cc} \qquad \text{S3}$$

where, $E_{ox}(D)$ represents the oxidation potential of the donor calculated based on effective mass approximation (0.922 V for InP and 1.47 V for CdSe), $E_{red}(A)$ is the reduction potential of the acceptor (-0.45 V) was obtained from literature.[6] E_{00} is the zero–zero excitation energy (smallest bandgap in the system) of the QDs (2.07 eV for InP and 2.14 eV for CdSe), e^2 is the electronic charge, ε_s is the solvent dielectric constant and d_{cc} is the center to center distance between the donor and acceptor. Since the center to center distance (d_{cc}) is large in the present case (>1.8 nm) the last term can be neglected. (Note: All the oxidation/reduction potentials presented are *vs* NHE).

8. Steady state emission studies

Three independent experiments using different sets of QDs were carried out for InP (B-D) and CdSe (F-H). Mean values are used for estimating the radius of quenching sphere and the Stern-Volmer plots.

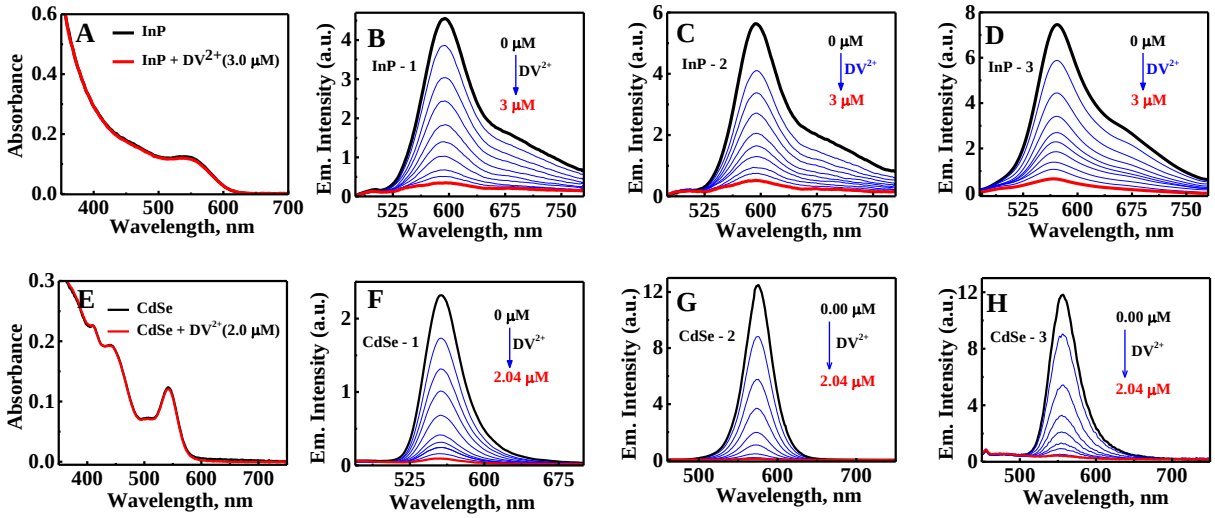

Figure S2. (A) Absorption spectrum of InP QDs in the absence (black trace) and presence of DV^{2+} (red trace) and (B-D) steady state emission changes of InP QDs (~0.40 μM) on addition of varying concentration of DV^{2+} (0-3.0 μM) in toluene containing 1% of methanol. (E) Absorption spectrum of CdSe QDs in the absence (black trace) and presence of DV^{2+} (red trace); (F-H) emission changes of CdSe QDs (~0.4 μM) on addition of varying concentration of DV^{2+} (0-2.04 μM) in toluene containing 1% of methanol.

8.1. Radius of quenching sphere

The relative emission intensities of unquenched to quenched InP QDs (I_0/I) showed an exponential relationship towards the higher concentration of DV^{2+}, as shown in equation S4,

$$I_0 / I = e^{\alpha[DV^{2+}]} \qquad \text{S4}$$

where α represents the quenching constant. The plot of $\log(I_0/I)$ versus the concentration of DV^{2+} showed a linear relationship and the α value was estimated to be 3.1 x 10^5 M^{-1}. From the Perrin analysis the quenching volume can be obtained as $\alpha = N_A * V$ where N_A is Avogadro number and V the quenching volume. Thus, from the α value obtained, the calculated quenching volume and radius is 5.2 x 10^{-16} cm^3 and 50 nm, respectively.

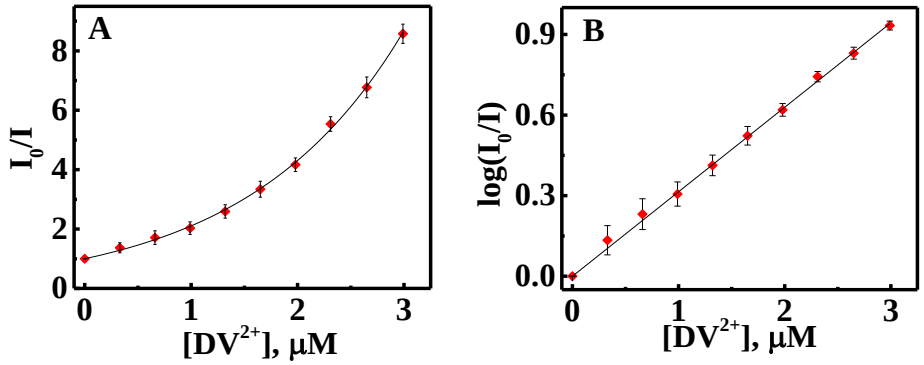

Figure S3. (A) Relative changes in the emission intensity of InP QDs upon the addition of DV^{2+} and (B) Plot for log (I_0/I) against varying concentrations of DV^{2+}.

9. Time resolved emission studies

Three independent experiments, using different sets of QDs, were carried out by exciting at 405 nm. Mean values of each component is used in the Stern-Volmer plots.

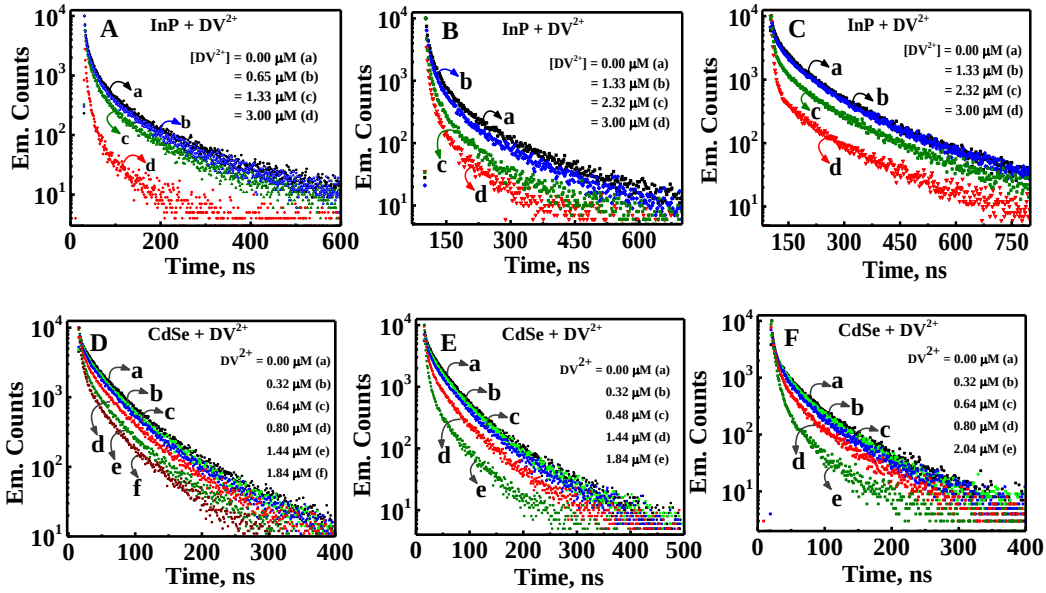

Figure S4. Emission decay profile of (A-C) InP QDs (~0.40 μM) monitored at 585 nm and (D-F) CdSe QDs (~0.40 μM) monitored at 558 nm at varying concentration of DV^{2+} in toluene containing 1% methanol. Three independent experiments, using different sets of QDs, were carried out by exciting at 405 nm.

Table S1. Fluorescence lifetimes and fractional contributions of InP QDs on addition of varying concentration of DV^{2+}

$[DV^{2+}]$, μM	τ_1 (ns)	a_1	τ_2 (ns)	a_2	τ_3 (ns)	a_3	τ_{avg} (ns)	χ^2
0	6.4	0.65	32.4	0.29	127.0	0.06	61.4	1.04
0.33	5.9	0.65	31.2	0.29	125.6	0.06	61.3	1.10
0.66	5.9	0.66	28.9	0.29	123.8	0.05	60.1	1.10
0.99	5.9	0.66	28.3	0.29	126.5	0.05	57.2	1.11
1.33	5.8	0.68	27.7	0.27	124.0	0.05	56.6	1.13
1.65	4.8	0.64	21.2	0.29	94.7	0.06	45.8	1.09
1.98	3.6	0.67	16.9	0.27	83.3	0.05	38.8	1.10
2.31	2.3	0.71	11.9	0.25	67.8	0.04	30.5	1.09
2.65	2.1	0.70	10.3	0.26	58.6	0.04	25.8	1.13
2.99	1.4	0.69	7.8	0.28	50.9	0.03	20.4	1.10

τ_1, τ_2 and τ_3 represent the lifetimes of individual components and a_1, a_2 and a_3 represent corresponding fractional contributions. τ_{avg} represents average lifetime calculated based on Equation S1. The quality of the fit is judged by statistical parameters such as χ^2 (1.00-1.15).

Table S2. Fluorescence lifetimes and fractional contributions of CdSe QDs on addition of varying concentration of DV^{2+}

$[DV^{2+}]$, μM	τ_1 (ns)	α_1	τ_2 (ns)	α_2	τ_3 (ns)	α_3	τ_{avg} (ns)	χ^2
0	2.9	0.76	21.2	0.18	57.9	0.06	30.4	1.13
0.16	2.9	0.72	19.1	0.21	57.4	0.07	30.9	1.00
0.32	3	0.69	18	0.23	55	0.08	30.4	1.03
0.48	3	0.7	19.1	0.23	56.7	0.07	30.1	1.16
0.64	3	0.74	18.1	0.2	57.1	0.06	28.9	1.10
0.80	2.9	0.76	16	0.19	52.3	0.05	24.4	1.04
0.96	2.9	0.73	14.6	0.21	47.8	0.06	23.4	1.03
1.12	2.9	0.83	10.8	0.13	42.5	0.03	15.0	1.03
1.44	1.8	0.79	6.4	0.19	34.5	0.02	10.3	1.10
1.76	1.7	0.85	5.7	0.14	29.7	0.01	6.2	1.00

τ_1, τ_2 and τ_3 represent lifetimes of individual components and α_1, α_2 and α_3 represent corresponding fractional contributions. τ_{avg} represents average lifetime calculated based in Equation S1 The quality of the fit is judged by statistical parameters such as χ^2 (1.00-1.16).

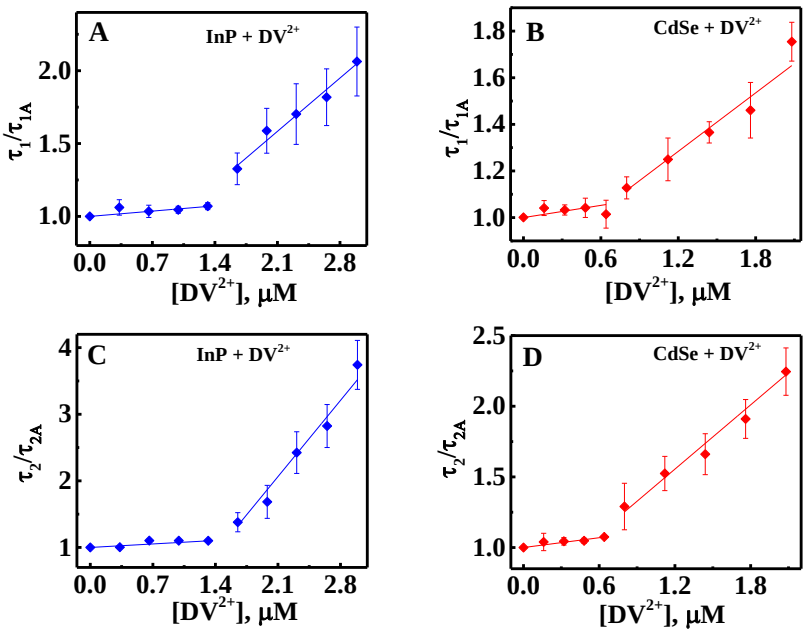

Figure S5: Relative changes corresponding to individual lifetime components of (A,C) InP QDs and (B,D) CdSe QDs as a function of varying concentration of DV^{2+}. τ_1 and τ_2 represents the individual lifetime in the absence and τ_{1A} and τ_{2A} represents lifetime in the presence of DV^{2+} (Three independent experiments using different sets of QDs were carried out by exciting at 405 nm and mean values are plotted with standard deviations).

Table S3. Average number of DV^{2+} (λ in the quenching sphere of InP QDs as a function of quencher concentration

$[DV^{2+}]$, μM	λ Value		
	Expt. No 1	**Expt. No 2**	**Expt. No 3**
0.33	0.16	0.24	0.31
0.66	0.40	0.53	0.52
0.99	0.62	0.79	0.73
1.32	**0.97**	**0.95**	**0.98**
1.65	1.18	1.17	1.24
1.98	1.49	1.41	1.45
2.31	1.91	1.68	1.79
2.65	2.19	1.93	2.02
2.99	2.56	2.45	2.38

Table S4. Average number of DV^{2+} (λ) in the quenching sphere of CdSe QDs as a function of quencher concentration

$[DV^{2+}]$, μM	λ Value		
	Expt. No 1	**Expt. No 2**	**Expt. No 3**
0.16	0.29	0.28	0.29
0.32	0.57	0.52	0.53
0.48	0.83	0.76	0.82
0.64	**1.12**	**1.05**	**1.06**
0.80	1.75	1.74	1.35
1.12	1.49	2.18	1.62
1.44	1.98	2.79	2.00
1.76	2.25	3.32	2.37
2.04	3.11	3.54	2.74

10. Zeta potential studies

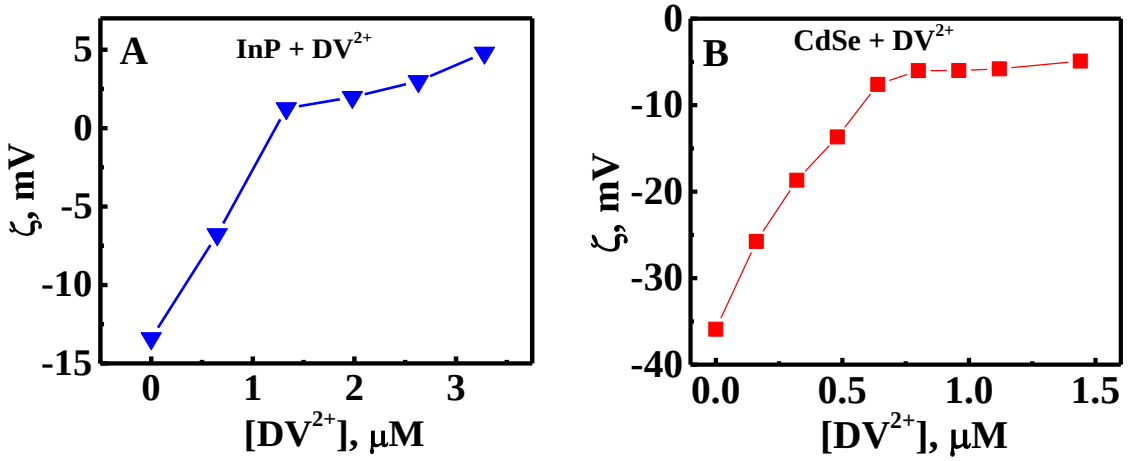

Figure S6. Variation of ζ (A) InP QDs and (B) CdSe QDs on addition of varying concentration of DV^{2+} (note: since the experiments were carried out in toluene, the relative variation in ζ is significant than the absolute values).

11. Transient absorption studies

11.1. Control experiments

We have performed control experiments to rule out the role of trace amount of methanol (1%) used to dissolve DV^{2+} and/or the counter ion (Br^-) in the formation of $DV^{+\bullet}$ and charge hopping process. Exchange of Br^- by PF_6^- allowed the elimination of methanol from the solvent mixture and dissolve DV^{2+} in a mixture of (1:50) acetonitrile and toluene. The kinetics of bleach recovery of InP QDs as well as the stability of the viologen radical remained more or less same as in the earlier case (Figure S8).

(a) In the absence of InP QDs

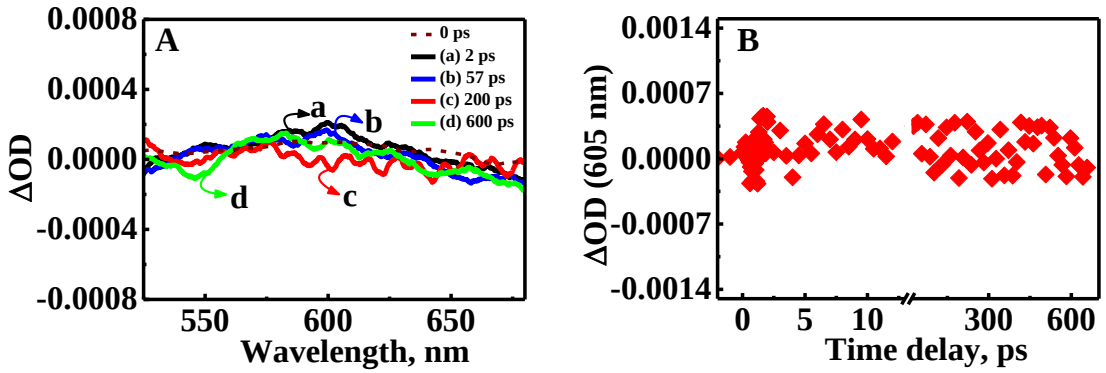

Figure S7. (A) Femtosecond transient absorption spectra and (B) Absorption-time profile of DV^{2+} (200 μM, four times the concentration of DV^{2+} used in the presence of InP QDs) in toluene containing 1% methanol, excited at 400 nm in the absence of InP QDs. The absorption-time profile was monitored at 605 nm.

(b) Using PF_6^- as counter ion and eliminating methanol

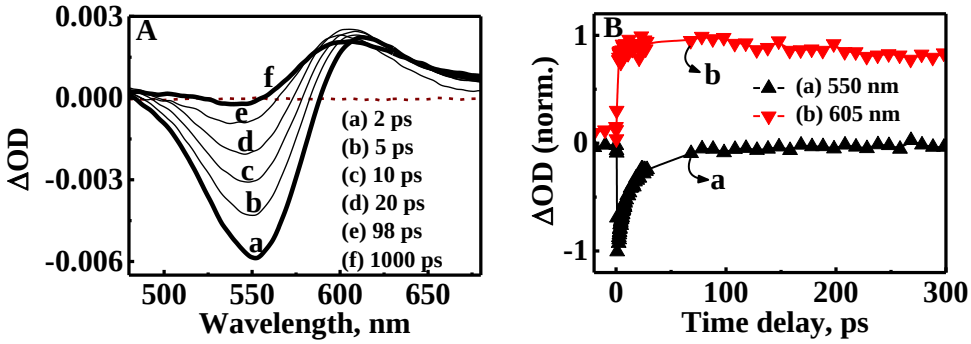

Figure S8. Femtosecond transient absorption studies of InP QDs in the presence of DV^{2+} with PF_6^- as counter ion (InP-DV^{2+}:$2PF_6^-$). (A) Transient absorption spectra of InP-DV^{2+}:PF_6^- (traces a-f) upon excitation at 400 nm and (B) absorption-time profile of InP-DV^{2+}:$2PF_6^-$ corresponding to fast bleach recovery at 550 nm (black trace a) and formation of $DV^{+\cdot}$ monitored at 605 nm (red trace b).

11.2. Transient absorption spectrum of CdSe in the presence of DV^{2+}

The higher intensity of $DV^{+\bullet}$ at lower time scales observed in Figure S9 can be attributed to the hot electron transfer from CdSe to DV^{2+}.[7]

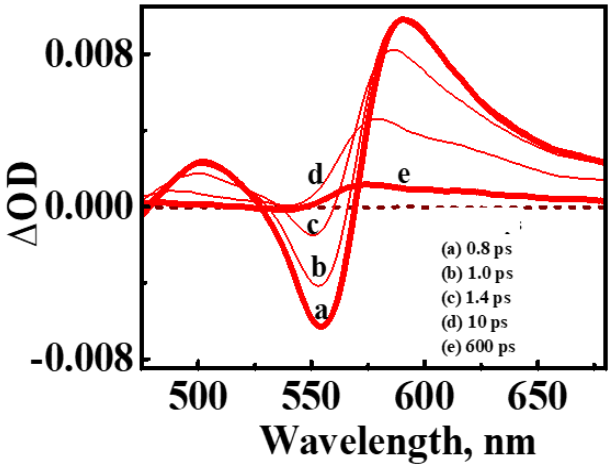

Figure S9. Femtosecond transient absorption spectra of CdSe QDs (9 μM) in the presence of DV^{2+} (30 μM) upon excitation at 400 nm.

11.3. Comparison of the nanosecond transient absorption of InP-DV^{2+} and CdSe-DV^{2+}

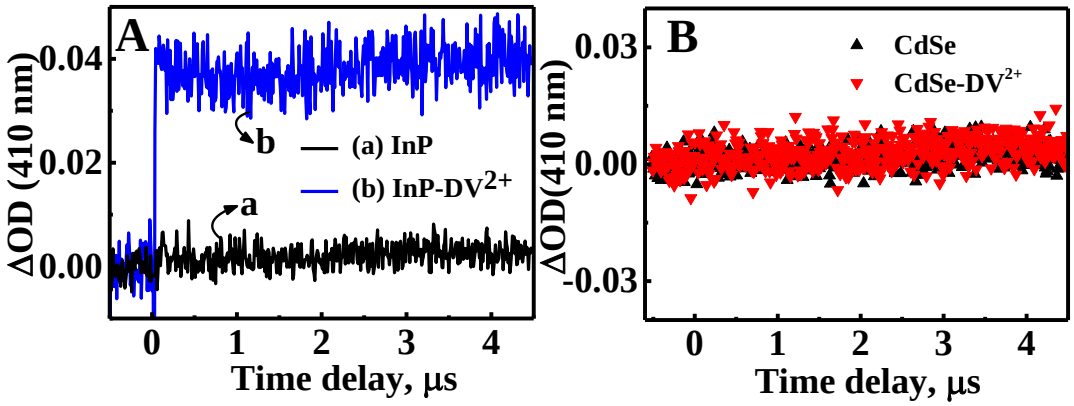

Figure S10. Nanosecond transient absorption studies of InP-DV^{2+} and its comparison with CdSe-DV^{2+}. (A) Absorption time profile of InP QDs (0.47 μM) in the absence (black trace a) and presence of DV^{2+} (5.3 μM; blue trace b) recorded at 410 nm. The positive absorption in InP-DV^{2+} corresponds to the absorption of $DV^{+\cdot}$. (B) Absorption time profile of CdSe (black trace) and CdSe-DV^{2+} (red trace) recorded at 410 nm. All the experiments were done in degassed toluene and excited at 355 nm.

11.4. Nanosecond transient absorption studies by varying the probe volume

The contribution of diffusion on the decay kinetics of viologen radical in nanosecond laser flash photolysis studies was found to be insignificant based experiment carried out by varying the probe diameter and its contribution towards the decay kinetics. The details of the experiment was given in Table S5. All the experimental conditions like laser power, concentration of DV^{2+} (13 μM) were kept identical for these experiments.

Table S5: Influence of probe diameter on the decay of viologen radical

Probe diameter (cm)	Lifetime (s)
0.2	2.0 ± 0.2
0.4	1.9 ± 0.2
0.6	1.8 ± 0.2

12. STELLA Simulation

Kinetics of the back electron transfer involving hopping, in the case of InP-DV^{2+}, was obtained using STELLA programme, a kinetic modeling programme used to simulate the hopping of viologen derivatives in zeolite cages.[8,9] A kinetic model was setup using the STELLA programme, and the experimental curve in the 4 ms time window (when λ>>1) was reproduced by fixing the back electron transfer rate same as when λ=1.

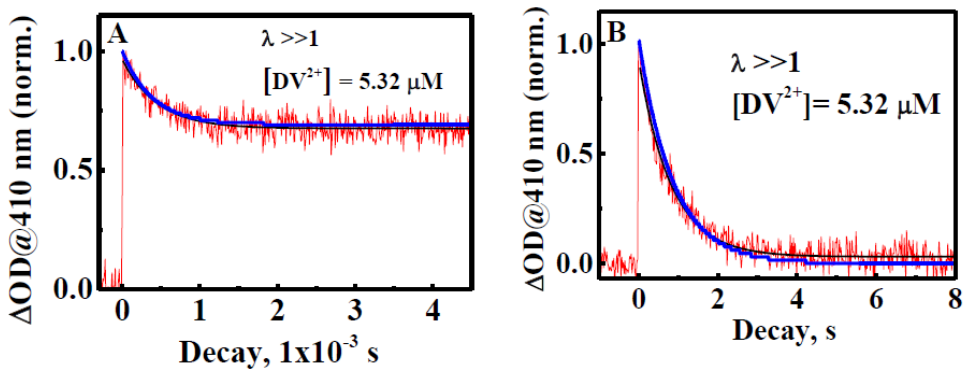

Figure S11: Absorption time profile of $\mathbf{DV^{+\bullet}}$ and the corresponding simulated fit using Stella programme when λ>>1. (A) in 4 ms time window and (B) in 8 s time window. The experimental fit is given as black solid line and simulated fit is given as blue solid line in both the Figures.

13. Quantum yield of $DV^{+\bullet}$

Quantum yield of $DV^{+\bullet}$ ($\Phi_{DV+\bullet}$), observed by following the decay in millisecond timescale for the InP based system, is estimated using C_{60} in toluene as an actinometer.[10,11] An optically matched solution of InP QDs and C_{60} at the laser excitation wavelength (OD = 0.6 at 355 nm) is used for the experiments. The quantum yield of $DV^{+\bullet}$ ($\Phi_{DV+\bullet}$) with respect to absorbed photons is calculated using the equation S5,

$$\Phi_{DV^{+\bullet}} = \Phi_T \frac{A_{DV^{+\bullet}} \times \varepsilon_{C_{60}}}{A_{C_{60}} \times \varepsilon_{DV^{+\bullet}}} \times 100 \quad \text{S5}$$

where Φ_T is the quantum yield of the C_{60} triplet (taken as unity), $A_{DV^{+\bullet}}$ is the differential absorbance of the reduced decyl viologen at 400 nm in the presence of InP QDs and $\varepsilon_{DV^{+\bullet}}$ is the extinction coefficient of viologen radical at 400 nm (42100 M^{-1} cm^{-1}).[12] $A_{C_{60}}$ is the absorbance corresponding to the triplet of C_{60} at 750 nm, and $\varepsilon_{C_{60}}$ is the extinction coefficient for the triplet of C_{60} at 750 nm (12000 M^{-1} cm^{-1}).

14. References

1. Patterson, A. L., The Scherrer Formula for X-Ray Particle Size Determination. *Phys. Rev.* **1939**, *56*, 978-982.

2. Jackson, K. A.; Schroter, W., *Handbook of Semiconductor Technology; John Wiley & Sons, Inc., Hoboken, NJ, USA* **2008**.

3. Moreels, I.; Lambert, K.; Muynck, D. D.; Vanhaecke, F.; Poelman, D.; Martins, J. C.; Allan,G.; Hens, Z. Composition and Size-Dependent Extinction Coefficient of Colloidal PbSe Quantum Dots *Chem. Mater.* **2007**, *19*, 6101-6106.

4. Burda, C.; Green, T. C.; Link, S.; El-Sayed, M. A. Electron Shuttling Across the Interface of CdSe Nanoparticles Monitored by Femtosecond Laser Spectroscopy. *J. Phys. Chem. B* **1999**, *103*, 1783−1788.

5. Blackburn, J. L.; Selmarten, D. C.; Nozik, A. J. Electron and Hole Transfer from Indium Phosphide Quantum Dots *J. Phys. Chem. B* **2003**, *107*, 14154−14157

6. Harris, C.; Kamat, P. V., Photocatalysis with CdSe Nanoparticles in Confined Media: Mapping Charge Transfer Events in the Subpicosecond to Second Timescales. *ACS Nano* **2009,** *3*, 682-690.

7. Jiang, Z. J.; Kelley, D. F. Hot and Relaxed Electron Transfer from the CdSe Core and Core/Shell Nanorods. *J. Phys. Chem. C* **2011**, *115*, 4594−4602.

8. Zhang, H.; Rajesh, C. S.; Dutta, P. K., Ruthenium Polypyridyl Complexes Containing a Conjugated Ligand LDQ (LDQ = 1-[4-(4′-methyl)-2,2′-bipyridyl]-2-[4-(4′-N,N′-tetramethylene-2,2′-bipyridinum)]ethene): Synthesis, Characterization, and Photoinduced Electron Transfer at Solution−Zeolite Interfaces. *J. Phys. Chem. C* **2009,** *113*, 4623-4633.

9. Vitale, M.; Castagnola, N. B.; Ortins, N. J.; Brooke, J. A.; Vaidyalingam, A.; Dutta, P. K., Intrazeolitic Photochemical Charge Separation for $Ru(bpy)_3^{2+}$−Bipyridinium System: Role of the Zeolite Structure. *J. Phys. Chem. B* **1999,***103*, 2408-2416.

10. Stamplecoskie, K. G.; Chen, Y. S.; Kamat, P. V. Excited-State Behavior of Luminescent Glutathione-Protected Gold Clusters. *J. Phys. Chem. C* **2014,** *118*, 1370-1376.

11. Stamplecoskie, K. G.; Kamat, P. V. Size-Dependent Excited State Behavior of Glutathione-Capped Gold Clusters and Their Light-Harvesting Capacity. *J. Am. Chem. Soc.* **2014,** *136,* 11093-11099.

12. Watanabe, T.; Honda, K. Measurement of the Extinction Coefficient of the Methyl Viologen Cation Radical and the Efficiency of its Formation by Semiconductor Photocatalysis. *J. Phys. Chem.* **1982,** *86,* 2617-2619.